Environ. Sci. Technol. **2006**, *40,* 1469−1477

Mechanism and Kinetics of Cyanogen Chloride Formation from the Chlorination of Glycine

CHONGZHENG NA AND
TERESE M. OLSON*

Environmental and Water Resource Engineering, Department of Civil and Environmental Engineering, University of Michigan, Ann Arbor, Michigan 48109-2125

Glycine is an important precursor of cyanogen chloride (CNCl)—a disinfection byproduct (DBP) found in chlorinated drinking water. To model CNCl formation from glycine during chlorination, the mechanism and kinetics of the reaction between glycine and free chlorine were investigated. Kinetic experiments indicated that CNCl formation was limited by either the decay rates of *N,N*-dichloroglycine or a proposed intermediate, *N*-chloroiminocarboxylate, $ClN{=}CHCO_2^-$. Only the anionic form of *N,N*-dichloroglycine, $NCl_2CH_2CO_2^-$, however, decays to form CNCl, while the protonated neutral species forms *N*-chloromethylimine. At pH > 6, glycine-nitrogen is stoichiometrically converted to CNCl, while conversion decreases at lower pH due to the formation of *N*-chloromethylimine. Under conditions relevant to drinking water treatment, i.e., at pH 6 to 8 and with free chlorine in excess, a simplified rate expression for the concentration of glycine-nitrogen converted to CNCl, $[CNCl]_f$, applies:

$$\frac{d[\mathrm{CNCl}]_f}{dt} = k_2^*[\mathrm{Cl_2\text{-}Gly}]_{T,o}\exp(-k_2^* t)$$

where $[Cl_2\text{-}Gly]_{T,o}$ is the initial concentration of total *N,N*-dichloroglycine, k_2^* is the first-order decay constant for $ClN{=}CHCO_2^-$, $k_2^*(s^{-1}) = 10^{12(\pm 4)}\exp(-1.0(\pm 0.3) \times 10^4/T)$, and T is the absolute temperature in K. Kinetic expressions for $d[CNCl]/dt$ when free chlorine is in excess, however, must also account for the significant decay of CNCl by hypochlorite-catalyzed hydrolysis, which has been characterized in previous studies. Although CNCl formation is independent of the free chlorine concentration, higher chlorine concentrations promote its hydrolysis.

Introduction

Cyanogen chloride (CNCl, CAS 506-77-4) is a disinfection byproduct (DBP) found in drinking water treated with free chlorine and chloramines at levels of several micrograms per liter (*1*). Recent studies, including model system investigations of CNCl yields (*2*) and precursor analysis studies with chlorinated river water in our laboratory, have identified the amino acid glycine (NH_2CH_2COOH, CAS 56-40-6) as an important CNCl precursor during chlorination. In each of these studies, it has been demonstrated that CNCl yields from glycine in the presence of free chlorine are complicated functions of its formation and decay rates. The CNCl decay mechanism due to hypochlorite-catalyzed hydrolysis has been well-characterized (*3*−*6*). Conversely, the CNCl formation mechanism from glycine, especially under the conditions of actual chlorination processes, is not well understood.

The reaction of glycine and free chlorine has primarily been studied with *glycine* in excess. Under these conditions, glycine is rapidly chlorinated to *N*-monochloroglycine ($NHClCH_2COOH$) by the electrophilic attack of HOCl on $NH_2CH_2COO^-$ (*7*−*9*). *N*-monochloroglycine is stable with a half-life of over 45 h (*10*) around neutral pH. The products of *N*-monochloroglycine decomposition were identified as formaldehyde and ammonia (*7*, *10*). Hand et al. (*10*) proposed that the decay occurred via concerted fragmentation and through the reaction intermediate methylimine ($HN{=}CH_2$).

In drinking water disinfection, *free chlorine*, rather than glycine, is usually present in excess. The excess free chlorine is expected to immediately chlorinate *N*-monochloroglycine to *N,N*-dichloroglycine (*7*, *11*). *N,N*-dichloroglycine, explosive in its pure form (*12*), is much less stable than *N*-monochloroglycine. Sawamura et al. (*13*) reported that the primary product of *N,N*-dichloroglycine decay was cyanide (CN^-). They observed a CN^- yield of at least 20% with 50 μM glycine and 75 μM free chlorine ($[Cl_2]_T$:$[Gly]_o \approx 1.5$) at pH 7 after 30 min. When free chlorine is present, cyanide is quickly chlorinated to cyanogen chloride. Gerritsen and Margerum (*14*) measured the second-order CNCl formation rate constant as $1.22 \times 10^9\ M^{-1}s^{-1}$ with respect to $[CN^-]$ and [HOCl] at 25 °C. Preliminary experiments in this research showed that CNCl formation from glycine was much slower than its formation from cyanide. We hypothesized, therefore, that the former reaction kinetics are essentially determined by the rate of cyanide formation from *N,N*-dichloroglycine decay.

Few studies of the mechanism of *N,N*-dichloroglycine decay have been reported. Analogies may be drawn, however, from the results of other α-amino acid chlorination investigations. A review of available chlorination studies of isoleucine (*15*), valine (*16*), phenylalanine (*17*), lysine (*18*), tyrosine (*19*, *20*), and aspartic acid (*20*) indicated that nitriles, aldehydes, and *N*-chloroaldimines have been found as products. By extension, the analogous chlorination products for glycine would be cyanide, formaldehyde, and *N*-chloromethylimine ($ClN{=}CH_2$).

At least two pathways to nitrile formation are proposed in the above amino acid chlorination studies. According to some investigators, *N*-chloroaldimine intermediates can dechlorinate to form nitriles, as well as aldehydes (*15*, *19*). An alternative path for nitrile formation was said to proceed directly from the decay of *N,N*-dichloroglycine (*16*−*18*, *20*, *21*), or through an alternate *N*-chlorocarboxylimine intermediate (*22*). In the case of glycine, therefore, possible pathways for cyanide formation (and thus CNCl), might be represented by pathways A and B, respectively, in Scheme 1. It is unclear, however, which steps govern the formation rate of CNCl.

On the basis of the literature, it was not yet possible to model the kinetics of CNCl formation from glycine under solution conditions relevant to actual chlorination processes. To develop such a model, the objective of this research was to elucidate the mechanism of *N,N*-dichloroglycine decay and CNCl formation. In combination with previous kinetic models we developed for the hypochlorite-catalyzed hydrolysis of CNCl (*3*), this formation mechanism provides a more complete foundation for estimating maximum CNCl concentrations that could be formed from glycine during chlorination. Given the time scale of these reactions, it was

* Corresponding author e-mail: tmolson@umich.edu.

10.1021/es0512273 CCC: $33.50
Published on Web 02/02/2006

SCHEME 1 . Pathways of Glycine Chlorination Proposed in the Literature

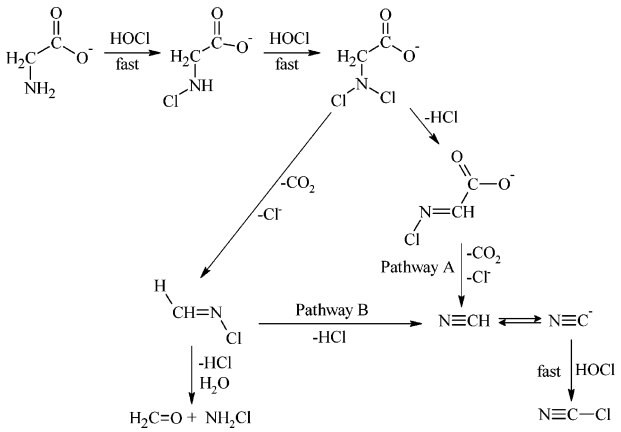

convenient to apply a real-time analysis technique, known as in-line membrane introduction mass spectrometry (MIMS). The method was particularly useful in distinguishing the importance of the two pathways (A and B in Scheme 1), as one of the proposed intermediates, *N*-chloromethylimine, could be monitored simultaneously with CNCl.

Materials and Methods

Reagents. All chemicals used in this study were ACS reagent grade. Glycine was obtained from Alfa Aesar (98.5+%). Sodium hypochlorite (4−6%) used as free chlorine, and potassium cyanide (KCN) used to generate CNCL standards, were purchased from Fisher Scientific. Sodium phosphate salts and hydrochloric acid (6 N) used to prepare buffer solutions were purchased from Sigma-Aldrich. All stock solutions were prepared with distilled, deionized (DI) water and stored in a refrigerator for no more than two weeks, with the exception of hypochlorite stock solutions which were prepared fresh and standardized by UV absorption at 292 nm ($\epsilon_{OCl,max} = 350\ M^{-1}cm^{-1}$, 25 °C, and pH > 9.5) (*23*) before use. Aqueous CNCl standard solutions were prepared as needed by utilizing the 1:1 stoichiometric reaction of KCN and NaOCl in phosphate buffer (*3*, *24*).

In−Line Membrane Introduction Mass Spectrometry. The primary analytical technique to monitor CNCl and *N*-chloromethylimine was in-line membrane introduction mass spectrometry. A detailed description of the reactor and MIMS detection system can be found in an earlier publication (*3*). A Hewlett-Packet 5972 quadruple mass spectrometer with electron impact ionization was used as the detector. The detection limit for cyanogen chloride was approximately 0.09 μM (S/N = 3).

Because the time scale of CNCl formation was comparable to the mass transfer rate through the MIMS membrane, it was necessary to consider and correct for a slight mass transfer lag in the analysis by modeling the transient diffusion of CNCl through the membrane. Since CNCl decay and formation reactions involve nonvolatile species and ions (i.e., the *N,N*-dichloroglycine anion for CNCl formation as discussed later herein and hypochlorite ions for decay) that do not significantly permeate the membrane, the membrane can be approximated as a purely diffusional domain with respect to CNCl transport. Membrane diffusivity coefficients in the MIMS were initially characterized using standard CNCl solutions. For these nonreactive solutions, CNCl transfer from the aqueous solution to the spectrometer was modeled as a pervaporation process (*25*). The tubular membrane was idealized as a hollow rod and the CNCl concentration in the membrane was assumed to vary in the radial, but not axial, direction according to the following governing transport equation and boundary and initial conditions (*26*):

$$\frac{1}{D_m}\frac{\partial C'}{\partial t} = \frac{\partial^2 C'}{\partial r^2} + \frac{1}{r}\frac{\partial C'}{\partial r} \tag{1}$$

$$\text{B.C.s:}\quad C'(r = r_i, t) = \frac{C_a(t)}{\sigma} \tag{2}$$

$$C'(r = r_o, t) = 0 \tag{3}$$

$$\text{I.C.:}\quad C'(r, t \le t_d) = 0 \tag{4}$$

where $C' = C/\alpha\sigma$, C = CNCl concentration in the membrane, α = partitioning coefficient between aqueous solution and the membrane, $\sigma = \ln(r_o/r_i)/2\pi l\varphi\tau D_m\alpha$, a calibration coefficient, l = length of tubular membrane, φ = mass spectrometer multiplier current gain, τ = time interval between measurements, D_m = diffusion coefficient in the membrane, r = radius from the center of tubular membrane with r_i and r_o being inner and outer radii, t = reaction time, C_a = bulk concentration in aqueous solution, and t_d = time needed to pump reaction solution from the reactor to the membrane. The ion abundance of CNCl on the MIMS detector side was calculated as

$$I(t) = -r_o \ln(r_o/r_i)\left.\frac{\partial C'}{\partial r}\right|_{r=r_o} \tag{5}$$

For a given measurement of $I(t)$, estimates of the corresponding $C_a(t)$ were obtained by numerically solving eqs 1−5 using values of D_m, t_d, and σ estimated from CNCl standards (*26*). The calculations were performed with Matlab 6.5 (student release). Details of the theory and approach to estimate these model parameters are described in the Supporting Information.

Experimental Procedures. The chlorination experiments were conducted in the in-line MIMS system in darkness. To start the reaction, glycine was mixed with NaOCl solution buffered with 100 mM phosphate and adjusted with hydrochloric acid. Cyanogen chloride and *N*-chloromethylimine were identified and monitored at their characteristic mass-to-charge ratios. To effect the formation of *N,N*-dichloroglycine and achieve a nearly constant free chlorine concentration, free chlorine was added at concentrations more than 15 times the glycine concentration. The excess free chlorine concentration also facilitated an accurate estimation of CNCl decay due to hypochlorite catalysis (*3*). After the initial instantaneous formation of *N,N*-dichloroglycine, the free chlorine concentration remained constant. This constant concentration, $[Cl_2]_T$, was calculated as the initial concentration added minus twice the initial glycine concentration.

The reaction mechanism of *N,N*-dichloroglycine decay was examined from pH 4 to 8 at 25 °C. The initial glycine concentration ranged from 1 to 15 μM. The effect of temperature on CNCl formation was further assessed at 15 and 35 °C.

Results and Discussion

Acquisition of Aqueous CNCl Concentration and Formation of Cyanogen Chloride. Cyanogen chloride was observed at its characteristic mass-to-charge ratios (m/z) of 61 ($CN^{35}Cl$) and 63 ($CN^{37}Cl$) (*2*, *3*). Ion counts at m/z 61 were used to represent CNCl abundance on the MIMS detector side:

$$I_{CNCl} = I_{CN^{35}Cl} = I_{m/z\ 61} \tag{6}$$

An example I_{CNCl} time profile, $I(t)$, multiplied by the MIMS calibration coefficient σ is provided in Figure 1 (in gray) for the conditions of 10 μM initial glycine ($[Gly]_o$) and 208 μM free chlorine ($[Cl_2]_T$) at pH 6.9 and 25 °C. Prior to estimating

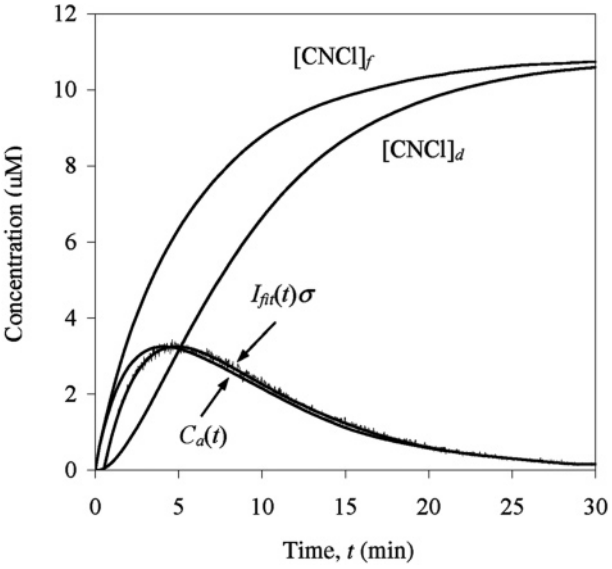

FIGURE 1. Example CNCl time profile observed with $[Gly]_o = 10\ \mu M$ and $[Cl_2]_T = 208\ \mu M$ at pH 6.9 and 25 °C. The raw experimental data are presented by $I(t)\sigma$ in gray. $I_{fit}(t)\sigma$ represents a polynomial fit to the raw data, $C_a(t)$ is the estimated aqueous CNCl concentration, $[CNCl]_d$ is the estimated concentration of CNCl that decayed by OCl^--catalyzed hydrolysis, and $[CNCl]_f$ is the "cumulative" concentration of CNCl formed.

the aqueous CNCl concentration time profile $C_a(t)$ on the reaction solution side of the membrane, the very large, noisy data sets were first fitted to smooth polynomial functions. These polynomial functions were subsequently represented as $I_{fit}(t)\sigma$, as shown in Figure 1, and used to solve eqs 1−5. Details of the solution method can be found in the Supporting Information. The resulting $C_a(t)$ solution is plotted in Figure 1 (solid black line) to demonstrate the effect of the mass transfer lag correction.

On the basis of our previous studies of the hypochlorite-catalyzed hydrolysis of CNCl (*3*), significant CNCl decay occurs in the presence of excess free chlorine. The "cumulative" concentration of cyanogen chloride formed, $[CNCl]_f$, therefore, was calculated as the sum of the actual CNCl concentration, C_a, and the hypothetical concentration of CNCl that decayed by OCl^--catalyzed hydrolysis, $[CNCl]_d$

$$[CNCl]_f = C_a + [CNCl]_d \tag{7}$$

Using the previously determined rate expression for the hydrolysis reaction (*3*)

$$\frac{d[CNCl]}{dt} = -k_{OCl}[OCl^-][CNCl] \tag{8}$$

and numeric integration, the $[CNCl]_d$ term was estimated as

$$[CNCl]_d = \int_{t=0}^{t} C_a k_{OCl}[OCl^-]dt \approx \sum_{t=0}^{t} C_a k_{OCl}[OCl^-]\tau \tag{9}$$

with $k_{OCl}\ (M^{-1}s^{-1}) = 5 \times 10^9 \exp(-5242/T)$ and T = absolute temperature in K. An example calculation of $[CNCl]_f$ is also shown in Figure 1.

Nitrogen Recovery Fraction. As shown in Figure 1, the formation of CNCl was typically complete in approximately 25 min at 25 °C. The maximum value of $[CNCl]_f$ may be referred to as $[CNCl]_{f,max}$. $[CNCl]_{f,max}$ was found to be proportional to $[Gly]_o$ at any given pH. This proportionality at pH 5.01(±0.04) is illustrated in Figure 2a. The slope of the linear relation between $[CNCl]_{f,max}$ and $[Gly]_o$ represents the *cumulative fraction of original glycine-nitrogen, θ, that was converted to cyanogen chloride-nitrogen,* a quantity that will be referred to hereafter as the *nitrogen recovery fraction*:

$$\theta = \frac{[CNCl]_{f,max}}{[Gly]_o} \tag{10}$$

For the example data set in Figure 2a, θ was estimated as 0.65(±0.01) according to eq 10. (The values in parentheses here and throughout this paper are standard deviations.)

Nitrogen recovery fractions were observed to vary as a function of pH. As shown in Figure 2b, θ increased monotonically with increasing pH over the pH range of 4 to 5.5, reached unity around pH 5.5 to 6, and remained near unity up to pH 8. Since glycine is rapidly converted to *N,N*-dichloroglycine when free chlorine is in excess, i.e.,

$$[Gly]_o = [Cl_2\text{-}Gly]_{T,o} \tag{11}$$

a value of $\theta \approx 1$ implies that the decay of *N,N*-dichloroglycine predominantly forms CNCl at pH > 6. As pH decreases, however, other decay pathways that do not yield CNCl become more important in order to explain the observation that $\theta < 1$.

The pH dependence of θ may be explained by speciation changes of *N,N*-dichloroglycine, namely

$$N^+HCl_2CH_2COOH \underset{H^+}{\overset{K_{a1}}{\rightleftharpoons}} NCl_2CH_2COOH \underset{H^+}{\overset{K_{a2}}{\rightleftharpoons}} NCl_2CH_2COO^- \tag{12}$$

Although the ionization constants K_{a1} and K_{a2} have not been experimentally characterized for *N,N*-dichloroglycine, analogies may be drawn from the ionization constants of *N*-monochloroalanine. From kinetic measurements, Stanbro and Smith (*27*) estimated the values of pK_{a1} and pK_{a2} for *N*-monochloroalanine as 2.5 and 5.4, respectively. Given the assumption that the pK_{a1} and pK_{a2} values for *N,N*-dichloroglycine are similar to those of *N*-monochloroalanine (this assumption will be justified by estimation later), the predominant species from pH 4 to 8 are neutral and anionic *N,N*-dichloroglycines. Since CNCl formation is favored at pH > 6, the carboxylate form of *N,N*-dichloroglycine appears to be the reactive precursor species. Decomposition of the neutral dichloroglycine species was hypothesized to produce other nitrogen-containing products and account for the decrease of θ at pH < 6. Kinetic studies of the reaction mechanism and experiments to identify intermediates were conducted to further test these hypotheses.

Kinetics of CNCl Formation. Given the above *N,N*-dichloroglycine speciation implications for CNCl formation, we additionally examined the kinetic relationship between CNCl formation and *N,N*-dichloroglycine decay. Assuming that decomposition of the anionic *N,N*-dichloroglycine form is a rate-limiting step for CNCl formation, and that first-order decay of the neutral *N,N*-dichloroglycine occurs in parallel, as follows:

$$NCl_2CH_2COOH \xrightarrow{k_1} \text{other products} \tag{13}$$

$$NCl_2CH_2COO^- \xrightarrow{k_2} CNCl + \text{other products} \tag{14}$$

the integrated time profile of $[CNCl]_f$ can be derived as

$$\ln\left(1 - \frac{[CNCl]_f}{[CNCl]_{f,max}}\right) = -k_{obs}t \tag{15}$$

where

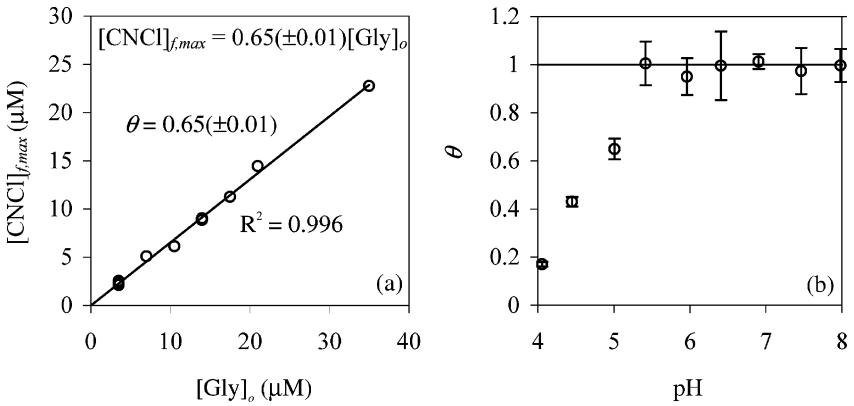

FIGURE 2. (a) Example linear relation between $[CNCl]_{f,max}$ and $[Gly]_o$ at pH 5.01 (±0.04) and 25 °C. (b) pH dependence of nitrogen recovery fraction.

$$k_{obs} = \frac{k_1[H^+] + k_2K_{a2}}{[H^+] + K_{a2}} \quad (16)$$

and k_1 and k_2 are first-order rate constants.

The hypothesized kinetic relationship for CNCl formation represented by eq 15 was tested by plotting $\ln(1 - [CNCl]_f/[CNCl]_{f,max})$ vs t at pH 6.9, where the expected predominant form of *N,N*-dichloroglycine was the anion form. The resulting plot is shown in Figure 3a. At this pH, and in fact at all pH > 6, linear relationships were observed, supporting the proposed reaction mechanism.

Mathematically, the expected effect of the parallel neutral *N,N*-dichloroglycine species decay (k_1) step on the kinetics of CNCl formation was to modulate the value of the observed first-order decay constant, k_{obs}, as described by eq 16. Linear plots similar to those obtained in Figure 3a, therefore, should be obtained at all pH according to the proposed mechanism. At pH < 6, however, deviations from linearity were observed at the early stage of CNCl formation, although it was noted that after the first 5 min, a linear relation was recovered. An example of this trend at pH 4.0 is shown in Figure 3b. To account for such deviations from linearity, some modifications to the proposed reaction mechanism were necessary.

The "early" deviations from pseudo-first-order kinetics observed at pH < 6 suggested that at least two rate-limiting steps, rather than one, were involved in CNCl formation. These pH conditions correspond to the same pH range in which a decrease in CNCl-nitrogen recovery, θ, was observed. Given this correspondence, we sought to determine whether the decay rate of carboxylate *N,N*-dichloroglycine had become apparently slower due to the growing importance of neutral *N,N*-dichloroglycine decay. In addition, the decay of carboxylate *N,N*-dichloroglycine was proposed to form a primary intermediate, *X*, whose decay is rate-limiting during the later stage of CNCl formation. These modifications to the mechanism required that reaction 14 be replaced with the following serial set of proposed rate-limiting reactions:

$$NCl_2CH_2COO^- \xrightarrow{k_2} X \quad (17)$$

$$X \xrightarrow{k_2^*} CNCl + \text{other products} \quad (18)$$

The kinetics of CNCl formation was then reexamined for consistency with the modified reaction scheme, particularly for reaction conditions at pH < 6.

Assuming a first-order decay rate constant of the intermediate, k_2^*, the following rate expression for CNCl formation can be derived (see the Supporting Information for derivation):

$$\frac{d[CNCl]_f}{dt} = \frac{k_2k_2^*K_{a2}[Cl_2\text{-Gly}]_{T,o}}{k_2K_{a2} + k_1[H^+] - k_2^*(K_{a2} + [H^+])}\left[\exp(-k_2^*t) - \exp\left(-\frac{k_2K_{a2} + k_1[H^+]}{K_{a2} + [H^+]}t\right)\right] \quad (19)$$

The corresponding integrated expression for CNCl formation is as follows:

$$\frac{[CNCl]_f}{[CNCl]_{f,max}} = \frac{1}{k_2^{*-1} - k_{obs}^{-1}}\left[\frac{1 - \exp(-k_2^*t)}{k_2^*} - \frac{1 - \exp(-k_{obs}t)}{k_{obs}}\right] \quad (20)$$

where the symbol k_{obs} is equal to its previous assignment in eq 16. When $k_2^* \ll k_{obs}$, eq 20 reduces to an equivalent form of eq 15

$$\ln\left(1 - \frac{[CNCl]_f}{[CNCl]_{f,max}}\right) = -k_2^*t \quad (21)$$

At pH > 6, therefore, the slopes of pseudo-first-order plots, such as the one in Figure 3a, provided estimates of k_2^*, which was $3.0(\pm0.1) \times 10^{-3}$ s^{-1} in this example. The linear region (at t > 5 min) in plots of $\ln(1 - [CNCl]_f/[CNCl]_{f,max})$ vs t at pH < 6, as shown in Figure 3b, yielded similar slopes. This suggests that eq 21 can be used to describe the kinetics after the initial deviation period.

Estimates of k_2^* were found to be independent of both free chlorine concentration and pH. For instance, with a variation of $[Cl_2]_T$ from 25 to 1000 μM at pH 5.01(±0.04), the average k_2^* value was estimated as $2.8(\pm0.1) \times 10^{-3}$ s^{-1}. From pH 4 to 8, over a four-order of magnitude change in proton concentration, little variation in k_2^*, estimated as $3.0(\pm0.3) \times 10^{-3}$ s^{-1}, was observed. (See the Supporting Information for data plots.)

To fully test the proposed mechanism and resulting rate expression for CNCl formation, i.e., eq 20, nonlinear regressions of the data to the model were performed at pH < 6. Using the previously estimated value of k_2^* and kinetic data from 0 to 30 min, k_{obs} was obtained from a single-parameter nonlinear least-squares fit of eq 20. A typical fit of the model to the data in Figure 3b is illustrated in Figure 4a, wherein $k_{obs} = 1.13(\pm0.02) \times 10^{-2}$ s^{-1}. The pH dependence of this parameter, as described by eq 16, and the intrinsic parameters upon which it depends were subsequently evaluated.

To estimate all of the intrinsic parameters in eq 16, k_1, k_2, and K_{a2}, it was necessary to consider the pH dependence of both k_{obs} and θ, since k_2 and K_{a2} cannot be estimated independently from the expression of k_{obs} alone. According

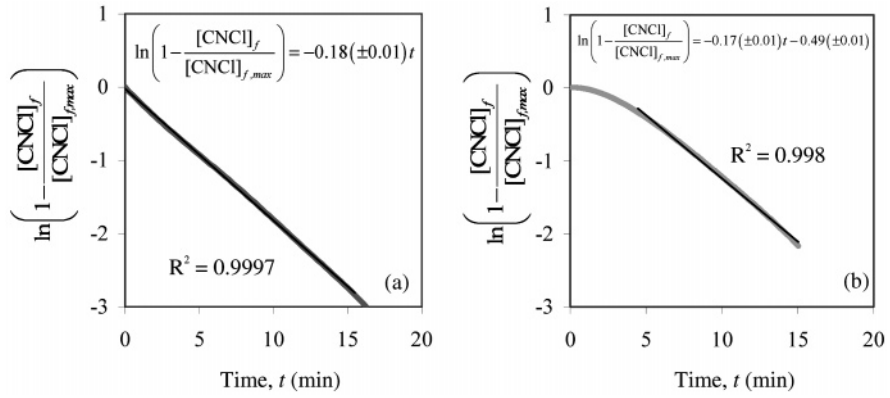

FIGURE 3. Test of the proposed reaction mechanism represented by eq 15. (a) An example at pH > 6. (b) An example at pH < 6. Experimental data are shown in gray and the black line is a linear regression of the data to eq 15. A linear regression of the data in (a) demonstrated that the *y*-intercept term was not statistically significant from zero. The data in (b), at times longer than 5 min, however, had a significant nonzero intercept. Experimental conditions in (a) are the same as those shown in Figure 1. Experimental conditions in (b) are $[Gly]_o$ = 10 μM and $[Cl_2]_T$ = 423 μM at pH 4.0 and 25 °C.

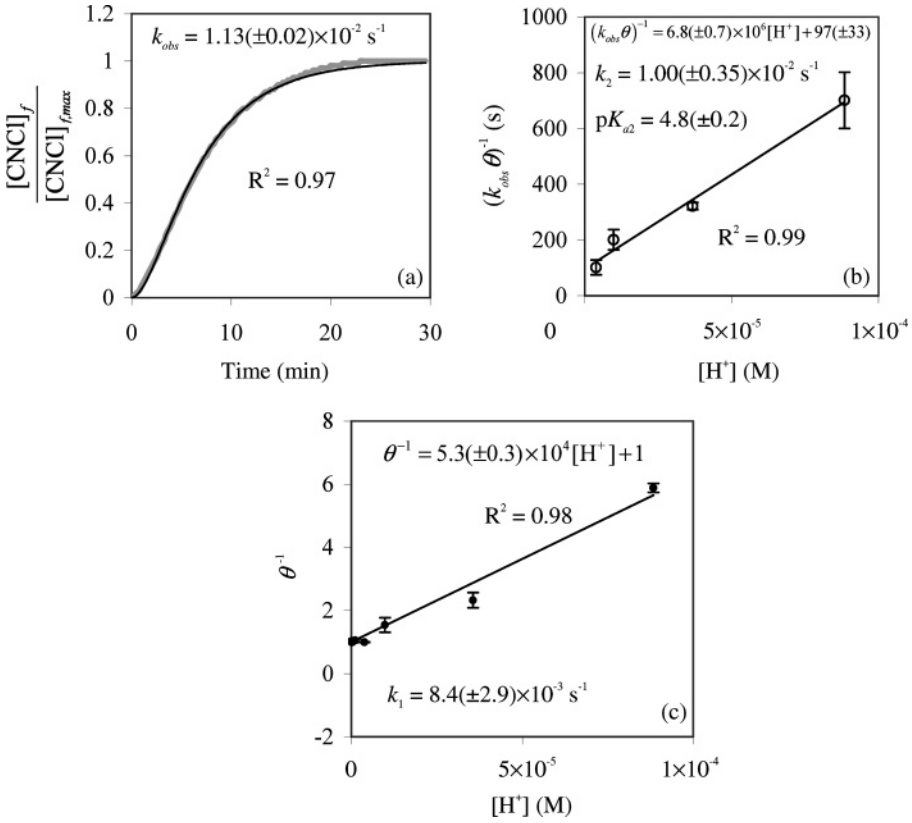

FIGURE 4. (a) Estimation of k_{obs} for the experiment shown in Figure 3b. (b) Estimation of k_2 and pK_{a2} using k_{obs} values estimated at pH 4–5.5. (c) Estimation of k_1 using the data presented in Figure 2b.

to the proposed mechanism of reactions 13 and 14, the nitrogen recovery fraction, θ, would have the following expected pH dependence:

$$\theta = \frac{k_2K_{a2}}{k_1[H^+] + k_2K_{a2}} \tag{22}$$

Combining eqs 16 and 22 yields the following linear expression in terms of [H$^+$]:

$$(k_{obs}\theta)^{-1} = \frac{[H^+]}{k_2K_{a2}} + \frac{1}{k_2} \tag{23}$$

A plot of $(k_{obs}\theta)^{-1}$ vs [H$^+$] using measured values of k_{obs} and θ from pH 4 to 5.5 yielded a linear relationship, as illustrated in Figure 4b. Linear regressions were performed to obtain estimates of k_2 and K_{a2}. At 25 °C, $k_2 = 1.00(\pm0.35) \times 10^{-2}$ s^{-1} and pK_{a2} (M) = 4.8(±0.2). A separate linearization of eq 22 provided a means to estimate k_1 where

$$\theta^{-1} = \frac{k_1[H^+]}{k_2K_{a2}} + 1 \tag{24}$$

As shown in Figure 4c, a plot of θ^{-1} vs [H$^+$] is also linear and provides an estimate of $k_1 = 8.4(\pm2.9) \times 10^{-3}$ s^{-1} (25 °C) based on a linear regression value of the slope and previous estimates of k_2 and K_{a2}.

The estimated pK_{a2} was comparable to that of *N*-monochloroalanine as discussed earlier. pK_{a2} can also be

estimated using correlations such as Taft's equation. Brown et al. (*28*) suggested an approach that regarded chlorinated amino acids as chloramine substitution on aliphatic acid backbone. For *N,N*-dichloroglycine, the backbone structure is acetic acid and the following Taft equation should be used:

$$pK_{a2} = 4.76 - 0.67\sigma^* \quad (25)$$

Brown et al. suggested that the Taft parameter σ^* be calculated based on the substituent value for $-NH_2$ ($\sigma^* = 0.62$) plus the value for chlorine substitution. The value of σ^* for chlorine substitution was obtained by drawing analogies from $-CH_3$, $-CH_2Cl$, $-CHCl_2$, and $-CCl_3$, where σ^* increased 0.9 for each chlorine substitution. Applying these assumptions to *N,N*-dichloroglycine, $\sigma^* = 0.62 + 2 \times 0.9 = 2.42$. Substitution of this value in eq 25 gave $pK_{a2} = 3.14$. Similarly, pK_{a2} was estimated as 3.48 using the ACD/I-Lab service (ACD/pK_a v 8.02), which is also based on Taft's correlation. Both the values estimated using Taft's correlation were significantly lower than the pK_{a2} value estimated from kinetic data in this study. However, a similar finding was also reported for *N*-monochloroalanine, in which the estimated pK_{a2} using Taft's equation (*28*) was 1.8 pH units lower than the value obtained from kinetic models (*27*). The significant overestimation of *N*-chloro amino acid acidity by the Taft correlation suggests that assumptions of similar electronic effects of chlorine substitution at $-NH_2$ and $-CH_3$ are probably flawed.

Formation and Decay of *N*-Chloromethylimine. One possible candidate for the product of carboxylate *N,N*-dichloroglycine decay and the intermediate of HCN formation was proposed as *N*-chloromethylimine, as shown in Pathway B in Scheme 1. In this study, *N*-chloromethylimine was observed at its characteristic mass-to-charge ratios of 63 ($CH_2{=}N^{35}Cl^+$) and 65 ($CH_2{=}N^{37}Cl^+$). Since CNCl is also characterized by a mass spectral peak at m/z 63, the abundance of *N*-chloromethylimine was calculated as the total intensity at m/z 63 less the intensity due to CNCl

$$I_{CH_2=NCl} = I_{CH_2=N^{35}Cl^+} = I_{m/z\,63} - 0.3I_{m/z\,61} \quad (26)$$

We did not select m/z 65 to represent $CH_2{=}NCl$ because its intensity was only $^1/_3$ of the $CH_2{=}NCl$ intensity at m/z 63. Using the intensity of m/z 65 would have lead to a noisier data set.

N-chloromethylimine is very unstable, so it was not possible to prepare standards for MIMS calibration. The calibration coefficient $\sigma = \ln(r_o/r_i)/2\pi l\varphi\tau D_m\alpha$ depends on the membrane diffusivity coefficient, D_m. For cyanogen chloride, both D_m and σ were found to be independent of pH (*29*). *N*-chloromethylimine, like CNCl, is a neutral molecule with no pH-dependent speciation, and hence it is reasonable to assume that its diffusivity in the membrane and its instrument calibration coefficient are similarly pH independent. It was assumed in this study, therefore, that $I_{CH_2=NCl}$ is proportional to the *N*-chloromethylimine concentration over the experimental conditions of pH 4−8.

Observed trends in $I_{CH_2=NCl}$ revealed both formation and decay processes, as shown in the semilog scale plot of Figure 5. After approximately 7 min, a linear relation between ln $I_{CH_2=NCl}$ and t was observed, suggesting pseudo first-order decay kinetics

$$\ln I_{CH_2=NCl} = \ln I_{CH_2=NCl,o} - k_1^* t \quad (27)$$

where $I_{CH_2=NCl,o}$ = intensity extrapolated to $t = 0$ and k_1^* = decay rate constant. The slope of the linear relation provided an estimate of $k_1^* = 2.5(\pm0.1) \times 10^{-3}$ s^{-1}. Values of k_1^* under other experimental conditions showed that k_1^* was independent of both free chlorine concentration and pH. The average of k_1^* equaled $2.7(\pm0.2) \times 10^{-3}$ s^{-1} from pH 4 to 5.5 at 25 °C.

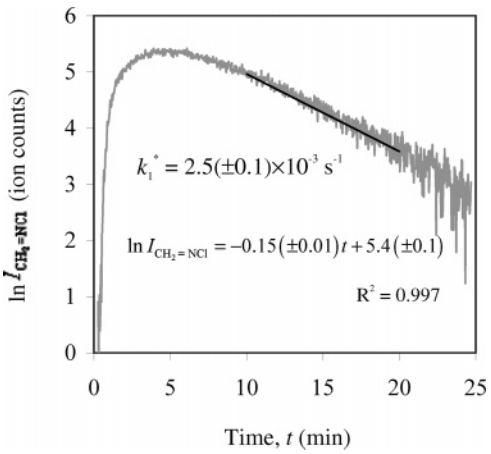

FIGURE 5. Formation and decay of *N*-chloromethylimine during the chlorination of glycine. The light line is experimental data and the black line represents a polynomial fit to the data over the portion used in the regression to obtain k_1^*. $[Gly]_o = 20$ μM and $[Cl_2]_T = 845$ μM at pH 4.4 and 25 °C.

The decomposition of *N*-chloromethylimine probably produced formaldehyde (CH_2O) and monochloramine (NH_2Cl). Under the experimental conditions, i.e., with Cl_2 in large excess, any NH_2Cl formed during the reaction would be rapidly converted to trichloramine (NCl_3). We did observe spectral peaks corresponding to NCl_3 with time by MIMS, but were unable to quantify it in our experiments. *N*-chloromethylimine decay, however, may not be the only source of NCl_3 because CNCl decay itself also produces NCl_3 (*3*).

Although the decay rate of *N*-chloromethylimine was independent of pH, absolute values of $I_{CH_2=NCl}$ were pH dependent. Example time profiles of $I_{CH_2=NCl}$ with [Gly] ≈ 10 μM are presented in Figure 6. From pH 7.5 to 5.0, with decreasing pH, the peak intensity (and hence concentration) of $CH_2{=}NCl$ increased. This trend was opposite to the observed pH dependence of θ, which is a measure of CNCl formation. If $CH_2{=}NCl$ was an intermediate of the CNCl formation pathway, $CH_2{=}NCl$ would have to decay faster at higher pH than at lower pH in order to form more CNCl at higher pH and observe less intermediate. Since the decay constant, k_1^*, was shown to be pH-independent, however, *N*-chloromethylimine cannot be a CNCl precursor intermediate. We propose instead that *N*-chloromethylimine is an intermediate of the parallel neutral dichloroglycine species decay pathway.

Further decreases in pH from 5.0 to 4.0 resulted in decreasing peak intensities of $CH_2{=}NCl$. This trend could be explained by the protonation of neutral *N,N*-dichloroglycine to form the cationic species, which was either nonreactive or decayed to form products other than $CH_2{=}NCl$ or CNCl. Corresponding pK_{a1} values for *N,N*-dichloro amino acids have not been characterized, however.

Mechanism of CNCl Formation. A mechanism for *N,N*-dichloroglycine decay and CNCl formation consistent with the data presented above is shown in Scheme 2. According to this reaction scheme, the neutral *N,N*-dichloroglycine species decomposes to form *N*-chloromethylimine. *N*-chloromethylimine is also unstable and probably hydrolyzes to form formaldehyde and monochloramine. The anionic *N,N*-dichloroglycine is proposed as the reactive species to form CNCl through an intermediate. Decay of the intermediate itself, however, is likely to form HCN initially, which would react rapidly to form CNCl. Since the formation of

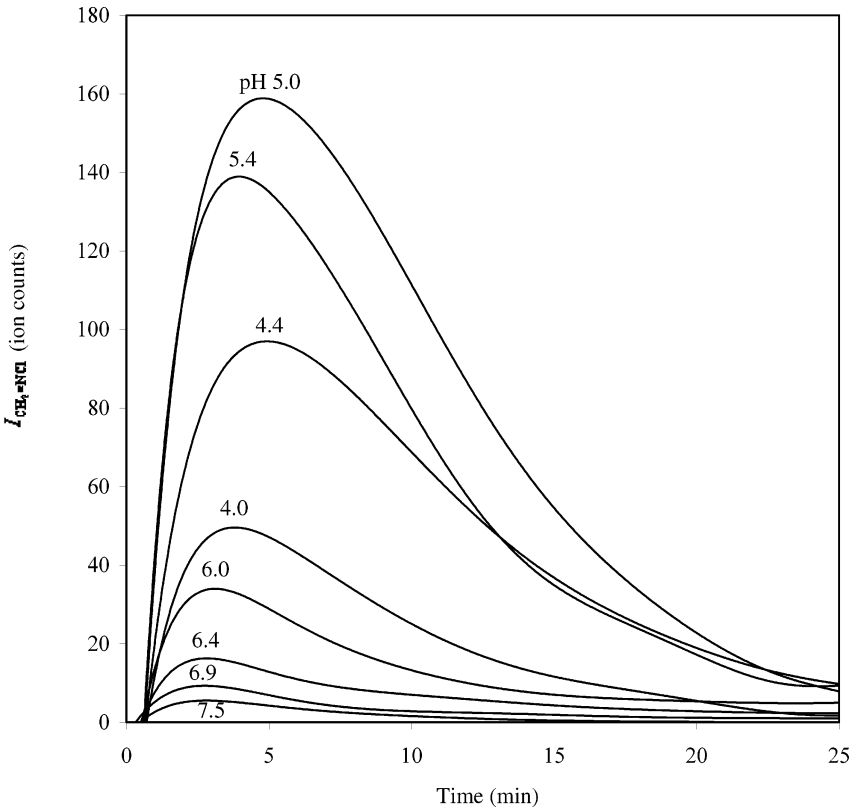

FIGURE 6. pH dependence of *N*-chloromethylimine abundance during the chlorination of glycine. $[Gly]_o \approx 10\ \mu M$ and free chlorine in excess at 25 °C.

SCHEME 2 . Proposed Pathways of *N,N*-Dichloroglycine Decay

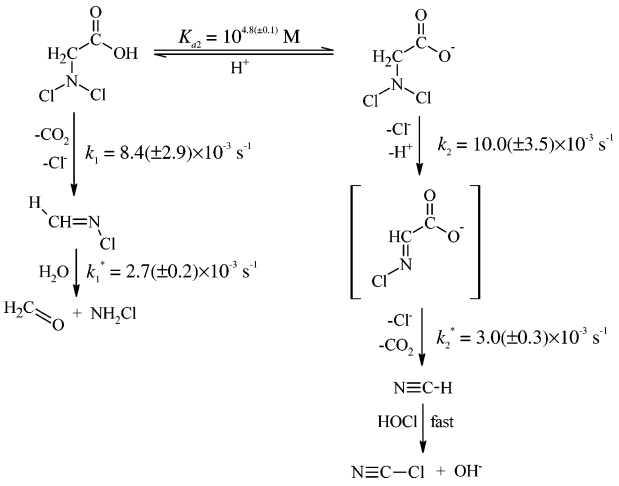

HCN requires the elimination of carboxylate, α-hydrogen, and both chlorine atoms, and since CO_2 and chlorine are not eliminated first (otherwise the intermediate would be CH_2=NCl), a likely intermediate is *N*-chloroiminocarboxylate. Due to the polar nature of this compound, however, it would not be identifiable directly by MIMS. The equilibrium and rate constants at 25 °C are also presented in Scheme 2.

The decomposition of monochloro amino acids has been proposed to occur by concerted fragmentation (*10*). The concerted fragmentation of a compound requires that its electron-withdrawing and electron-donating groups become antiperiplanar to each other. The two leaving groups in *N*-monochloroamino acids are chlorine and carboxylate. Results obtained from theoretical calculations using both semiempirical and ab initio methods supported the concerted fragmentation mechanism (*30*, *31*). The transition state structure had reduced dihedral angles of Cl−C and N−COO^-, suggesting that the *p* orbitals that these leaving groups occupied were skewed to achieve maximal overlap and facilitate the formation of the new π bond.

Our results, however, suggest that more than one fragmentation pathway exists for *N,N*-dichloroamino acids. According to our proposed mechanism, the two different pathways are essentially determined by the presence of a proton. When the carboxyl group is deprotonated, *N,N*-dichloroglycine decay leads to CNCl formation that may be explained by concerted fragmentation. In this case, the first fragmentation proceeds by eliminating one chlorine and one α-hydrogen to form *N*-chloroiminocarboxylate. A second fragmentation occurs by eliminating the remaining chlorine and carbon dioxide. To explain the formation of CH_2=NCl from the decomposition of neutral *N,N*-dichloroglycine, the cyclic transition state shown here involving the carboxylic proton, as proposed by Brown et al. (*28*) for *N*-monochloroalanine decay, may facilitate the immediate decarboxylation of *N,N*-dichloroglycine:

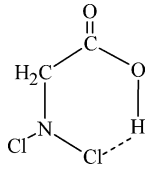

Temperature Dependence of CNCl Formation. In addition to the above determinations at 25 °C, the rate constant for CNCl formation, k_2^*, was also measured at 15 and 35 °C at pH 7. At pH 7, the kinetics of CNCl formation can be represented by eq 21. Linear regression provided the estimates of k_2^* at these temperatures. The temperature dependence of k_2^* could be modeled with the following linearized Arrhenius Equation (see the Supporting Information for details):

$$k_2^*(s^{-1}) = 10^{12(\pm 4)} \exp\left(-\frac{1.0(\pm 0.3) \times 10^4}{T}\right) \quad (28)$$

On the basis of this analysis, the activation energy for the decomposition of *N*-chloroiminocarboxylate anion is E_a = 82(±24) kJ/mol.

Implications for Drinking Water Disinfection. The proposed mechanism of CNCl formation from glycine implies that as long as free chlorine is in sufficient excess at the beginning of disinfection, any naturally occurring glycine is rapidly chlorinated to *N,N*-dichloroglycine. The subsequent relatively slow decay of *N,N*-dichloroglycine to produce hydrogen cyanide is independent of free chlorine concentration. Once *N,N*-dichloroglycine is formed, strategies such as reducing free chlorine or replacing free chlorine with chloramines, therefore, will not help to reduce this source of cyanide production. Consequently, since both free chlorine and chloramines react rapidly with cyanide to form CNCl (*32*, *33*), such changes in disinfection practice are likely to be ineffective in controlling CNCl formation originating from glycine. In fact, since the presence of free chlorine can catalyze the hydrolysis of CNCl while chloramines do not, post conversion of free chlorine to chloramines after disinfection may serve to *stabilize* CNCl. These factors may in part explain why the highest concentrations of CNCl are generally associated with drinking water utilities with combined use of Cl_2 and chloramines (*1*).

CNCl formation is sensitive to temperature change. For example, at 25 °C the time for 90% of glycine to be converted to CNCl, $t_{90\%}$, is about 12 min. The value of $t_{90\%}$ increases to 44 min at 15 °C and 2.5 h at 5 °C. (The rate constant estimate at 5 °C was extrapolated based on the Arrhenius eq 28.) Thus, at warmer temperatures, CNCl formation is likely to be complete inside treatment facilities with common contact times of 15 to 60 min. However, at colder temperatures, CNCl will continue to form in the distribution system. This may, in part, explain the observation in some cases that CNCl concentrations increase in the distribution system (*1*).

CNCl formation is not sensitive to pH change as long as pH > 6. However, as we reported previously (*3*), CNCl decays through hypochlorite-catalyzed hydrolysis when free chlorine is present. Basic pH favors the speciation of hypochlorite and consequently the destruction of CNCl.

The relative importance of glycine as a CNCl precursor was also recently examined in chlorinated natural river water samples in our laboratory (*34*). Approximately 42−45% of the CNCl produced in these samples was estimated to be derived from glycine. Given the importance of glycine as a precursor in surface water supplies, the above-mentioned implications regarding the factors and disinfection strategies that influence CNCl formation from glycine, as revealed by the mechanism, are particularly consequential.

Currently there is no proposed specific maximum contaminant level (MCL) guideline value for CNCl in drinking water, however, the World Health Organization (WHO) has published recommendations regarding the limits for *total* cyanogen compounds, of which CNCl would be a component (*35*). The WHO guideline value is 70 μg/L as total cyanide. This concentration is about a factor of 10 higher than the typical drinking water concentrations of CNCl in utilities practicing chlorination with post-chloramination, where CNCl concentrations are typically highest. Future assessments of typical total cyanogen concentrations in such systems are needed, therefore, to determine whether the WHO guideline is generally satisfied and these would in turn determine whether the CNCl produced in these systems is problematic.

Acknowledgments

We thank the U.S. Environmental Protection Agency Science to Achieve Results (STAR) Program and the University of Michigan for providing funding to conduct this research. Although the research described in this article has been funded in part by USEPA through grant 82823103-0 to the University of Michigan, it has not been subjected to the Agency's required peer and policy review and therefore does not necessarily reflect the views of the Agency and no official endorsement should be inferred.

Note Added after ASAP Publication

There was an error in Figure 1 in the version published ASAP February 2, 2006; the corrected version was published ASAP February 8, 2006.

Supporting Information Available

Estimation of membrane diffusivity and calibration parameters, mass transfer correction procedures in kinetic experiments, Matlab code of $C_a(t)$ acquisition, sensitivity analysis of $C_a(t)$ estimation procedures, derivation of eqs 20 and 22, dependence of k_2^* on free chlorine concentration, pH, and temperature, and a list of notations. This material is available free of charge via the Internet at http://pubs.acs.org.

Literature Cited

(1) Krasner, S. W.; Mcguire, M. J.; Jacangelo, J. G.; Patania, N. L.; Reagan, K. M.; Aieta, E. M. The Occurrence of Disinfection Byproducts in United States Drinking Water. *J. Am. Water Works Assoc.* **1989**, *81*, 41−53.

(2) Shang, C.; Gong, W. L.; Blatchley, E. R. Breakpoint chemistry and volatile byproduct formation resulting from chlorination of model organic-N compounds. *Environ. Sci. Technol.* **2000**, *34*, 1721−1728.

(3) Na, C.; Olson, T. M. Stability of Cyanogen Chloride in the Presence of Free Chlorine and Monochloramine. *Environ. Sci. Technol.* **2004**, *38*, 6037−6043.

(4) Xie, Y. F.; Reckhow, D. A. In *AWWA Proceedings of 1992 Water Quality Technology Conference*; American Water Works Association: Toronto, ON, 1993.

(5) Bailey, P. L.; Bishop, E. Hydrolysis of cyanogen chloride. *J. Chem. Soc., Dalton Trans.* **1973**, *9*, 912−916.

(6) Price, C. C.; Larson, T. E.; Beck, K. M.; Harrington, F. C.; Smith, L. C.; Stephanoff, I. Hydrolysis and chlorinolysis of cyanogen chloride. *J. Am. Chem. Soc.* **1947**, *69*, 1640−1644.

(7) Sawamura, R.; Sakurai, E.; Kinosita, M.; Tachikawa, M.; Hasegawa, A. Mechanisms of Chloramine and Cyanogen Chloride Formation from Glycine. *Eisei Kagaku Japan. J. Toxicol. Environ. Health* **1982**, *28*, P38−P38.

(8) Margerum, D. W.; Gray, E. T.; Huffman, R. P. In *Organometals and Organometalloids*; ACS Symposium Series 82; American Chemical Society: Washington, DC, 1978; pp 278−291.

(9) Armesto, X. L.; Canle, M.; Santaballa, J. A. Alpha-Amino-Acids Chlorination in Aqueous-Media. *Tetrahedron* **1993**, *49*, 275−284.

(10) Hand, V. C.; Snyder, M. P.; Margerum, D. W. Concerted Fragmentation of *N*-Chloro-Alpha-Amino Acid Anions. *J. Am. Chem. Soc.* **1983**, *105*, 4022−4025.

(11) Sakurai, E.; Sawamura, R. The Reaction of Hypochlorite with Glycine. 2. The Mechanisms of the Formation of Chloroglycines and Their Decomposition. *Eisei Kagaku Japan. J. Toxicol. Environ. Health* **1983**, *29*, 368−375.

(12) Vit, J.; Barer, S. J. New Derivatives of Amino-Acids *N,N*-Dichloroglycine and *N,N*-Dichloro-B-Alanine. *Synth. Commun.* **1976**, *6*, 1−4.

(13) Sawamura, R.; Sakurai, E.; Kinosita, M.; Tachikawa, M.; Hasegawa, A. The Reaction of Hypochlorite with Glycine I. Decomposition of Glycine and Formation of Cyanogen Chloride. *Eisei Kagaku Japan. J. Toxicol. Environ. Health* **1982**, *28*, 267−273.

(14) Gerritsen, C. M.; Margerum, D. W. Nonmetal Redox Kinetics − Hypochlorite and Hypochlorous Acid Reactions with Cyanide. *Inorg. Chem.* **1990**, *29*, 2757−2762.

(15) Nweke, A.; Scully, F. E. Stable *N*-Chloroaldimines and Other Products of the Chlorination of Isoleucine in Model Solutions and in a Wastewater. *Environ. Sci. Technol.* **1989**, *23*, 989−994.

(16) McCormick, E. F.; Conyers, B.; Scully, F. E. *N*-Chloroaldimines. 2. Chlorination of Valine in Model Solutions and in a Wastewater. *Environ. Sci. Technol.* **1993**, *27*, 255−261.
(17) Conyers, B.; Scully, F. E. *N*-Chloroaldimines. 3. Chlorination of Phenylalanine in Model Solutions and in a Wastewater. *Environ. Sci. Technol.* **1993**, *27*, 261−266.
(18) Conyers, B.; Scully, F. E. Chloramines. 5. Products and implications of the chlorination of lysine in municipal wastewaters. *Environ. Sci. Technol.* **1997**, *31*, 1680−1685.
(19) Pereira, W. E.; Hoyano, Y.; Summons, R. E.; Bacon, V. A.; Duffield, A. M. Chlorination Studies. 2. Reaction of Aqueous Hypochlorous Acid with Alpha Amino Acids and Dipeptides. *Biochim. Biophys. Acta* **1973**, *313*, 170−180.
(20) Trehy, M. L.; Yost, R. A.; Miles, C. J. Chlorination Byproducts of Amino Acids in Natural Waters. *Environ. Sci. Technol.* **1986**, *20*, 1117−1122.
(21) Larson, T. E.; Weber, E. J. *Reaction Mechanisms in Environmental Organic Chemistry*; Lewis Publishers: Boca Raton, FL, 1994.
(22) Hureiki, L.; Croue, J. P.; Legube, B. Chlorination Studies of Free and Combined Amino Acids. *Water Res.* **1994**, *28*, 2521−2531.
(23) Morris, J. C. Acid Ionization Constant of HoCl from 5 to 35 Degrees. *J. Phys. Chem.* **1966**, *70*, 3798−3805.
(24) Wu, W. W.; Chadik, P. A.; Schmidt, C. J. An in situ Synthesis of Cyanogen Chloride as a Safe and Economical Aqueous Standard. *Water Res.* **1998**, *32*, 2865−2869.
(25) Kotiaho, T.; Lauritsen, F. R.; Choudhury, T. K.; Cooks, R. G.; Tsao, G. T. Membrane Introduction Mass-Spectrometry. *Anal. Chem.* **1991**, *63*, A875.
(26) Sysoev, A. A.; Ketola, R. A.; Mattila, I.; Tarkiainen, V.; Kotiaho, T. Application of the numerical model describing analyte permeation through hollow fiber membranes into vacuum for determination of permeation parameters of organic compounds in a silicone membrane. *Int. J. Mass Spectrom.* **2001**, *212*, 205−217.
(27) Stanbro, W. D.; Smith, W. D. Kinetics and Mechanism of the Decomposition of *N*-Chloroalanine in Aqueous Solution. *Environ. Sci. Technol.* **1979**, *13*, 446−451.
(28) Brown, M. C.; Lepree, J. M.; Connors, K. A. Pressure and pH dependence of the kinetics of decarboxylative dechlorination of *N*-chloro-L-alanine. *Int. J. Chem. Kinetics* **1996**, *28*, 791−797.
(29) Na, C. Formation of Cyanogen Chloride from Amino Acids and Its Stability with Free Chlorine and Chloramine. Ph. D. Dissertation, University of Michigan, Ann Arbor, MI, 2005.
(30) Andres, J.; Moliner, V.; Safont, V. S.; Domingo, L. R.; Picher, M. T. On transition structures for hydride transfer step in enzyme catalysis. A comparative study on models of glutathione reductase derived from semiempirical, HF, and DFT methods. *J. Org. Chem.* **1996**, *61*, 7777−7783.
(31) Queralt, J. J.; Safont, V. S.; Moliner, V.; Andres, J. Towards an understanding of the molecular mechanism of the unimolecular decomposition of the *N*-chloro-alpha-amino acids on the ground and excited states surfaces in aqueous medium. *Chem. Phys. Lett.* **1998**, *283*, 294−300.
(32) Gerritsen, C. M.; Gazda, M.; Margerum, D. W. Nonmetal Redox Kinetics − Hypobromite and Hypoiodite Reactions with Cyanide and the Hydrolysis of Cyanogen Halides. *Inorg. Chem.* **1993**, *32*, 5739−5748.
(33) Schurter, L. M.; Bachelor, P. P.; Margerum, D. W. Nonmetal Redox Kinetics − Monochloramine, Dichloramine, and Trichloramine Reactions with Cyanide Ion. *Environ. Sci. Technol.* **1995**, *29*, 1127−1134.
(34) Lee, J. H.; Na, C.; Olson, T. M.; Ramirez, R. L. Cyanogen Chloride Precursor Analysis in Chlorinated River Water. *Environ. Sci. Technol.* **2006**, *40*, 1478−1484.
(35) World Health Organization. *Guidelines for Drinking Water Quality*, 3rd ed.; WHO: Geneva, Switzerland, 2003.

Received for review June 27, 2005. Revised manuscript received December 21, 2005. Accepted December 23, 2005.

ES0512273